DOI: 10.1002/ejic.200800338

Compounds of Antibacterial Agent Ciprofloxacin and Magnesium – Crystal Structures and Molecular Modeling Calculations

Iztok Turel,*[a] Petra Živec,[a] Andrej Pevec,[a] Sarah Tempelaar,[b] and George Psomas*[c]

Keywords: Magnesium / Quinolone / Antibiotics / Crystal structure / Molecular modeling

Two novel magnesium complexes of the quinolone antibacterial drug ciprofloxacin (cfH) were isolated and their crystal structures determined. In both compounds, bidentate O,O′-bonding of quinolone molecules to the metal was observed and it was also found that a very extensive intermolecular hydrogen-bond framework is present. The structures of both compounds, $[Mg(H_2O)_2(cfH)_2](NO_3)_2{\cdot}2H_2O$ (**1**) and $[Mg(cfH)_3](SO_4){\cdot}5H_2O$ (**2**) respectively, were compared with previously isolated compounds $(cfH_2)_2[Mg(H_2O)_6](SO_4)_2{\cdot}6H_2O$ (**3**) and $[Mg(cf)_2]{\cdot}2.5H_2O$ (**4**) and the appearance of magnesium and quinolone in these structures was analyzed in detail. The lowest energy model structures of the new complexes were determined with molecular modeling calculations and compared with the corresponding structures of **1** and **2** determined by X-ray crystallography. Though we were not able to isolate the 1:1 magnesium–ciprofloxacin complex, modeling calculations were also performed for such a complex due to its possible importance in biological systems.

Introduction

Over the last few years quinolones have clinically been the most successful synthetic antibacterial agents[1–3] and one of the famous members of this large family—ciprofloxacin (cfH) (Scheme 1)—is a real blockbuster drug.

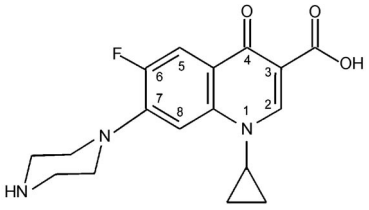

Scheme 1. Formula of ciprofloxacin [cfH = 1-cyclopropyl-6-fluoro-1,4-dihydro-4-oxo-7-(1-piperazinyl)-3-quinolinecarboxylic acid].

There is an unpredictable and never-ending battle between bacteria and mankind and diseases considered to be controlled or even eradicated are appearing again, often in new multidrug-resistant forms. A typical example is tuberculosis which is presently a worldwide health threat as resistant strains have slowly emerged.[4,5] Quinolones are used for the treatment of a variety of bacterial infections (and can be also considered for the treatment of tuberculosis). It is a fact that several pharmaceutical companies have left the antibiotic discovery field because they are much more interested in the more profitable areas of chronic diseases. Therefore, it is crucial to understand the molecular mode of action of existing drugs which could help us to exploit them even more efficiently in the future.

The selective activity of quinolones is through the inhibition of the supercoiling of DNA catalyzed by the bacterial enzyme DNA gyrase and metal ions are also involved in these processes. It is also known that quinolones can easily react with metal ions.[6] Several authors have studied metal–quinolone complexes and tested their interaction with biomolecules or biological activity.[6–10] On the one hand, metal–quinolone interactions are disturbing because the absorption of these drugs is reduced (because of the formation of sparingly soluble metal complexes) but on the other hand it is believed that metal ions are needed for the biological activity of quinolones. From all these facts it is obvious that it is extremely important to thoroughly reveal the details of these interactions.

Not many magnesium–quinolone crystal structures have been published in the literature[11–14] though it is clear that this metal is the most important for their activity.[15–17] It is not known yet whether the magnesium ion influence is due to its stabilizing effect on DNA topology or its ability to chelate with the keto and carboxylate moieties of quinolones.

[a] Faculty of Chemistry and Chemical Technology, University of Ljubljana,
Aškerčeva 5, 1000 Ljubljana, Slovenia
Fax: +386-1-2419220
E-mail: iztok.turel@fkkt.uni-lj.si
[b] Utrecht University, Department of Chemistry,
Utrecht, The Netherlands
[c] Department of General and Inorganic Chemistry, Faculty of Chemistry, Aristotle University of Thessaloniki,
P. O. Box 135, 54124 Thessaloniki, Greece
Fax: +30-2310997738
E-mail: gepsomas@chem.auth.gr
Supporting information for this article is available on the WWW under http://www.eurjic.org or from the author.

Theoretically, it is possible to design a huge number of magnesium–quinolone complexes—varying in metal–quinolone ratio (from 1:1 to 1:3), coordination mode, protonation of ligand and similar. However, among all the isolated metal–quinolone complexes the highest in number are 1:2 complexes with chelate (O,O′) bonding of the ligand via carboxylate and ring carbonyl oxygen atoms. Of course this does not preclude that less common forms could be the most important for biological activity.

In our efforts to isolate new compounds in the magnesium–ciprofloxacin system we have previously prepared an ionic compound $(cfH_2)_2[Mg(H_2O)_6](SO_4)_2{\cdot}6H_2O$[18] ($cfH_2$ is protonated quinolone) and polymeric $[Mg(cf)_2]{\cdot}2.5H_2O$.[12–13] However, up to now, we have not been able to prepare a discrete complex with two ciprofloxacin molecules coordinated to magnesium, though such complexes are common for other metals.[6]

Herein we report the synthesis and crystal structure of such a product—$[Mg(H_2O)_2(cfH)_2](NO_3)_2{\cdot}2H_2O$ (**1**). Moreover, we have additionally isolated $[Mg(cfH)_3](SO_4){\cdot}5H_2O$ (**2**)—where three molecules of ciprofloxacin are attached to the metal center. Both compounds are compared in detail with our previously published magnesium–ciprofloxacin complexes as well as with free quinolone molecules. Analysis of ciprofloxacin forms that are present in these structures is also given. This analysis could help to better understand the coordination between magnesium and ciprofloxacin and its possible influence in biological activity.

Additionally, molecular modeling techniques have been employed to assess the lowest energy model structure of each complex among all the possible isomers. The resultant model structures for complexes **1** and **2** have been compared with those determined by X-ray crystallography in an attempt to justify the formation of the final isomer. We were not able to isolate the 1:1 magnesium–ciprofloxacin complex though a complex with such a stoichiometric ratio could be important in biological systems.[19–20] Modeling calculations were performed for such a complex.

Results and Discussion

Syntheses

In our experiments aimed at preparing new compounds from magnesium–ciprofloxacin systems the conditions of the reactions were varied (systematically changing pH, solvent, metal–ligand ratio, type of metal salt). The mixing of aqueous solutions of metal salt and a quinolone mostly results in a precipitation, making it difficult to grow crystals of complexes. One of the reasons that crystallization is problematic is that a variety of sparingly soluble species are present in the solution mixture (differing in metal–ligand molar ratio from 1:1 to 1:3 and also differing regarding protonation and coordination modes).[21] It has been established that in these systems the use of hydrothermal reactions could lead to new crystalline products,[6,22] which was successfully proven also here in the isolation of new magnesium–ciprofloxacin products. However, in both procedures described herein only a small amount of crystals was prepared which enabled us to determine crystal structures and perform basic characterization. Attempts to obtain a satisfactory elemental analysis have proved to be unsuccessful, most probably due to facile solvent water loss. It has been shown before that weakly bonded lattice water molecules could easily be lost from metal–quinolone complexes already at room temperature.[23–27]

The polymeric 2D square grid complex $[Mg(cf)_2]{\cdot}2.5H_2O$ was isolated in our lab by hydrothermal reaction at neutral conditions (pH = 7)[13] but also earlier in the labs of a Chinese group at basic conditions (pH = 11).[12] Therefore, we decided to carefully lower the pH. We were aware that the pH should not be too low to prevent the protonation of quinolone. At pH = 6 a few crystals of $[Mg(cfH)_3](SO_4){\cdot}5H_2O$ (**2**) have grown together with a complex microcrystalline mixture.

In our attempts to prepare a heterometallic compound with a quinolone ligand, various combinations of metal salts (Cu^{II}, Zn^{II}, Mg^{II}) were used in reactions but no such product was isolated to date. However, in the hydrothermal reaction where magnesium and zinc salts were mixed with ciprofloxacin, surprisingly a new magnesium complex $[Mg(H_2O)_2(cfH)_2](NO_3)_2{\cdot}2H_2O$, (**1**) was isolated instead.

Description of Crystal Structures of $[Mg(H_2O)_2(cfH)_2](NO_3)_2{\cdot}2H_2O$ (1) and $[Mg(cfH)_3](SO_4){\cdot}5H_2O$ (2)

Crystal data and refinement parameters of compounds **1** and **2** are listed in Table 1.

The molecular structures of compounds **1** and **2** are shown in Figure 1 and Figure 2 and selected bond lengths and angles are collected in Table 2 and Table 3, respectively. All bond lengths and angles in both compounds are in agreement with corresponding data cited in the literature.[28,29]

Coordination of two quinolone ligands to magnesium occurs through the keto and carboxylate oxygen atoms. The aromatic ring systems of quinolone ligands are predominantly planar with the exception of the cyclopropyl group that sticks out of the plane whereas the piperazine rings are in the normal chair conformation. Quinolone ligands are in the zwitterionic form. In compound **1**, the slightly distorted octahedral coordination of magnesium is completed by two aqua ligands located in axial positions. The Mg–OH_2 distances [2.092(2) Å] are significantly longer than the equatorial Mg–O carboxylate/keto distances. The magnesium–carboxylate oxygen distance [2.039(2) Å] is very similar to the magnesium–keto oxygen distance [2.041(1) Å] which was also observed in structurally related magnesium complexes of levofloxacin and ofloxacin.[14] In the experimental charge density study of a copper–ciprofloxacin complex it was established that the asymmetry in the two C–O bond lengths of the carboxylate group [C(1)–O(11) and C(1)–O(12)] indicates that this is a partly localized carboxylate group.[20] The C(1)–O(11) bond is thus slightly longer and holds the majority of the negative charge, and consequently the metal–

Table 1. Crystal data and structure refinement for $[Mg(H_2O)_2(cfH)_2](NO_3)_2{\cdot}2H_2O$ (**1**) and $[Mg(cfH)_3](SO_4){\cdot}5H_2O$ (**2**).

	1	**2**
Formula	$C_{34}H_{44}F_2MgN_8O_{16}$	$C_{51}H_{64}F_3MgN_9O_{18}S$
Fw [g mol^{-1}]	883.08	1204.48
Crystal size [mm]	$0.45\times0.35\times0.13$	$0.25\times0.20\times0.15$
Crystal color	orange-brown	pale violet
Crystal system	triclinic	monoclinic
Space group	$P\bar{1}$	$P2_1/n$
a [Å]	9.3230(2)	13.7510(4)
b [Å]	10.0510(2)	16.8975(8)
c [Å]	11.9783(3)	23.415(1)
α [°]	76.3820(9)	90
β [°]	78.0642(9)	92.275(4)
γ [°]	63.8084(9)	90
V [Å^3]	972.03(4)	5436.4(4)
Z	1	4
T [K]	293	150
Calcd. density [g cm^{-3}]	1.509	1.472
F(000)	462	2528
θ Range [°]	2.55–27.48	1.02–25.03
No. of collected reflns.	7856	18690
No. of independent reflns.	4382	9588
R_{int}	0.018	0.029
No. of reflns. used	3555	7159
No. parameters	301	813
R [$I > 2\sigma(I)$][a]	0.0478	0.0439
wR_2 (all data)[b]	0.1377	0.1207
GoF, S[c]	1.030	1.032
Max./min. residual electron density [e Å^{-3}]	+0.518/–0.470	+0.948/–0.402

[a] $R = \Sigma||F_o| - |F_c||/\Sigma F_o|$. [b] $wR_2 = \{\Sigma[w(F_o^2 - F_c^2)^2]/\Sigma[w(F_o^2)^2]\}^{1/2}$. [c] $S = \Sigma[(F_o^2 - F_c^2)^2]/(n/p)]^{1/2}$ where n is the number of reflections and p is the total number of parameters refined.

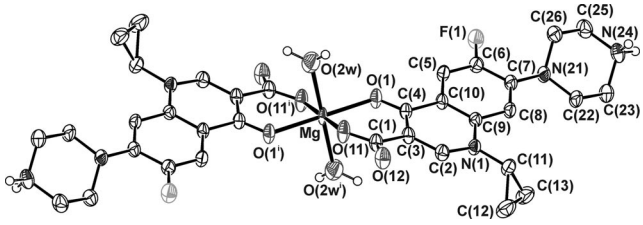

Figure 1. Atomic displacement plot (50% probability level) of the cation $[Mg(H_2O)_2(cfH)_2]^{2+}$ of **1**. The nitrate anions, lattice water molecules, and the hydrogen atoms on carbon atoms have been omitted for clarity.

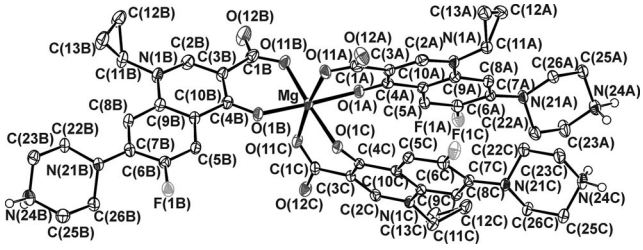

Figure 2. Atomic displacement plot (50% probability level) of $[Mg(cfH)_3]^{2+}$ of **2**. The sulfate anion, lattice water molecules, and hydrogen atoms on carbon atoms have been omitted for clarity.

Table 2. Selected bond lengths [Å] and angles [°] in $[Mg(H_2O)_2(cfH)_2](NO_3)_2{\cdot}2H_2O$ (**1**) [symmetry code: (i) $-x$, $-y + 1$, $-z$].

Mg–O(1)	2.041(1)
Mg–O(11)	2.039(2)
Mg–O(2w)	2.092(2)
C(1)–O(11)	1.262(2)
C(1)–O(12)	1.254(2)
C(4)–O(1)	1.259(2)
C(6)–F(1)	1.354(2)
O(11)–Mg–O(1)	86.04(5)
O(11)–Mg–O(2w)	88.85(8)
O(11)–Mg–O(1^i)	93.96(5)
O(11)–Mg–O(11^i)	180.0
O(11)–Mg–O(2w^i)	91.15(8)

Table 3. Selected bond lengths (Å) and angles (°) in $[Mg(cfH)_3](SO_4){\cdot}5H_2O$ (**2**).

Mg–O(1A)	2.102(2)
Mg–O(11A)	2.038(2)
Mg–O(1B)	2.066(2)
Mg–O(11B)	2.018(2)
Mg–O(1C)	2.113(2)
Mg–O(11C)	2.032(2)
C(1A)–O(11A)	1.272(3)
C(1A)–O(12A)	1.253(3)
C(1B)–O(11B)	1.266(3)
C(1B)–O(12B)	1.253(3)
C(1C)–O(11C)	1.256(3)
C(1C)–O(12C)	1.260(3)
C(4A)–O(1A)	1.261(3)
C(4B)–O(1B)	1.270(3)
C(4C)–O(1C)	1.265(3)
C(6A)–F(1A)	1.360(3)
C(6B)–F(1B)	1.367(3)
C(6C)–F(1C)	1.365(3)
O(11A)–Mg–O(1A)	84.39(7)
O(11C)–Mg–O(1B)	88.74(7)
O(11A)–Mg–O(1B)	95.05(7)
O(11C)–Mg–O(1A)	92.10(7)
O(11B)–Mg–O(1A)	91.46(7)
O(11A)–Mg–O(1C)	87.14(7)

O(11) bond is slightly shorter as is the metal–O(1) (ring keto) bond.

A detailed analysis of these structures shows a rich hydrogen-bonded framework which gives rise to two types of 12-member rings in the crystal structure (Figure 3 and Table S1). All these intensive interactions between coordinated and noncoordinated water molecules, nitrate anions, piperazine rings, and carboxylic groups stabilize the structure.

There is a slightly distorted octahedral coordination around the magnesium ion in the structure of **2** where three quinolone molecules are coordinated to the metal center. The bond lengths between quinolone carboxylate oxygen atoms (O11) and magnesium are substantially shorter [2.018(2)–2.038(2) Å] than those between ring keto (O1) and magnesium [2.066(2)–2.113(2) Å] (Table 3). The aro-

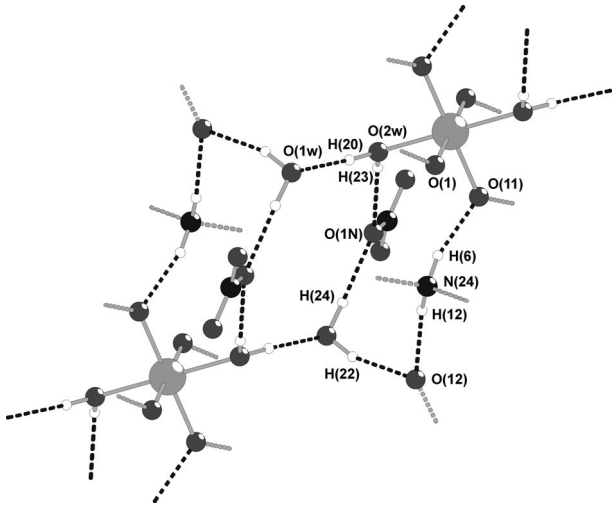

Figure 3. Part of the crystal structure of **1** showing O–H···O and N–H···O hydrogen bonds.

matic part of ciprofloxacin molecules (A, B, and C) is planar and the angles between neighboring molecules are 71.00(2)° (between A and B) and 75.16(3)° (between B and C), respectively. The aromatic quinolone parts of two ciprofloxacin ligands C from two neighboring $[Mg(cfH)_3]^{2+}$ cations in the crystal structure of **2** are parallel. Actually, the heterocyclic parts of quinolone rings are π–π stacked with centroid-to-centroid separation distances of 3.449(1) Å (Figure 4).

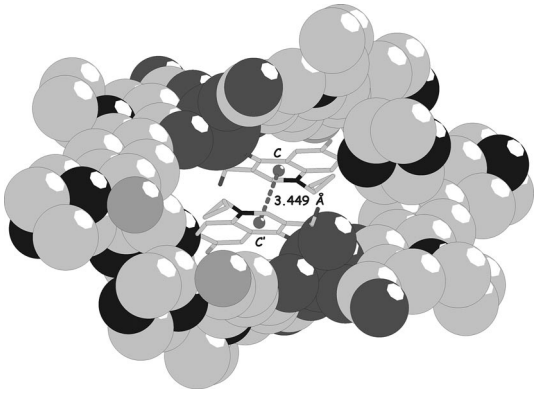

Figure 4. Schematic representation of the two neighboring cations $[Mg(cfH)_3]^{2+}$ of **2** (shown in space filling mode) showing the π–π stacked aromatic parts of ciprofloxacin molecules C. The centroid *C*···centroid *C′* distance is 3.449 Å.

Numerous O–H···O and N–H···O hydrogen bonds are present in the structure of **2** in which solvate water molecules and SO_4^{2-} anions are connected together and also with the piperazine rings and carboxylic groups of the $[Mg(cfH)_3]^{2+}$ cations. The details are shown in Figure 5 and Table S1. One piperazine ring nitrogen is involved in bifurcated N–H···O hydrogen bonds to the carboxylate oxygen atoms. Three lattice water molecules are linked into the chain with O···O distances of 2.786(3) and 2.751(3) Å. In biology, hydrogen-bonding involving water molecules along with other noncovalent interactions can play an important role in stabilizing the native conformation of the biomolecules and self-assembly processes.[30,31]

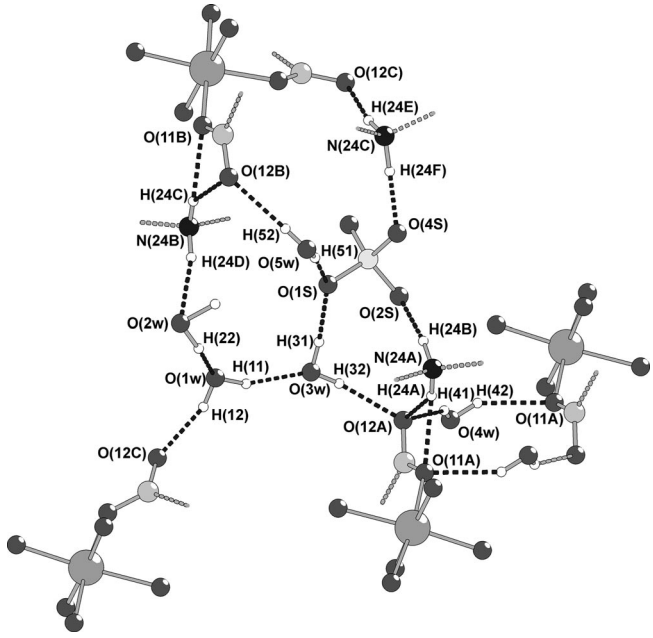

Figure 5. Part of the crystal structure of **2** showing O–H···O and N–H···O hydrogen bonds.

Analysis of Crystal Structures Containing Magnesium and Ciprofloxacin

Coordination Around Magnesium in Known Magnesium–Ciprofloxacin Compounds

In order to analyze the appearance of magnesium and quinolone we compared the structures of **1** and **2** with the previously isolated compounds $(cfH_2)_2[Mg(H_2O)_6](SO_4)_2 \cdot 6H_2O$ (**3**) and $[Mg(cf)_2] \cdot 2.5H_2O$ (**4**). Coordination geometry around the metal center in compounds **1**, **2**, **3**, and **4** is presented in Scheme 2 and bond lengths between magnesium and coordinated atoms are given in Table 4. In all these compounds, the coordination sphere around magnesium is octahedral. In **3**, quinolone is protonated and is not able to coordinate to magnesium.[18] Six aqua ligands are coordinated to the metal which is quite common for magnesium ions.[32]

Under hydrothermal conditions in basic medium a polymeric complex **4** forms.[12,13] Two quinolone molecules (in *trans* arrangement) are coordinated to magnesium through two oxygen atoms. Additionally, the terminal nitrogen atom of the piperazine ring, which is not protonated in basic conditions, is coordinated in the axial positions.

To the best of our knowledge apart from **2**, there are only two metal complexes structurally characterized with X-ray crystallography, where three quinolone molecules are

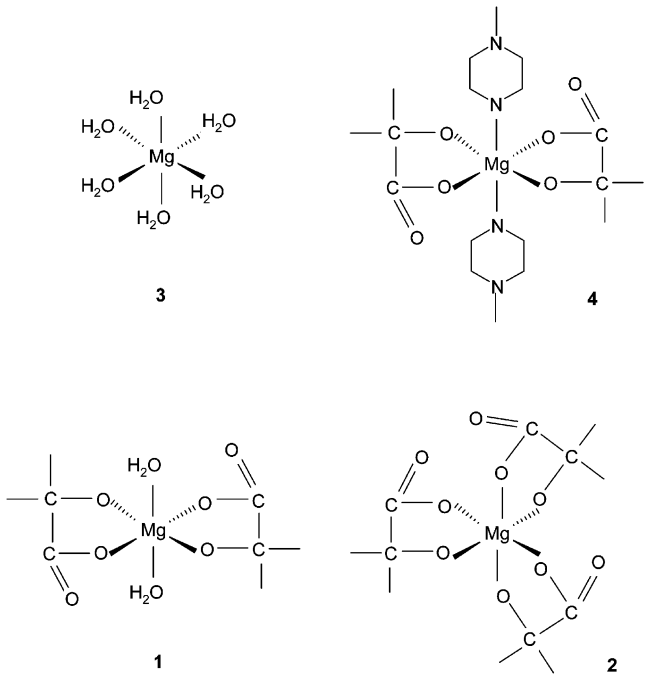

Scheme 2. Coordination sphere around magnesium ion in complexes **1**–**4**. Only the part of the quinolone molecule that is coordinated to metal is drawn.

Table 4. Bond lengths (Å) between magnesium and coordinated atoms in compounds **1**–**4**.

	1	**2**	**3**	**4**
Mg–O(1)	2.041(1)	2.066(2)–2.113(2)		2.053(1)
Mg–O(11)	2.039 (1)	2.018(2)–2.038(2)		2.041(1)
Mg–O(w)	2.092(2)		2.040(4)–2.063(5)	
Mg–N(24)				2.298(1)

coordinated to the metal ion (with coordination number 6), $Na[Co(cnx)_3]\cdot 6H_2O$[33] and $Na_2[(Cd(cnx)_3)(Cd(cnx)_3(H_2O))]\cdot 2H_2O$ (cnx is cinoxacin−a quinolone-family member), respectively.[34] Complex **2** was isolated at lower pH values than the mentioned cobalt and cadmium complexes. It is thus not surprising that zwitterionic ciprofloxacin is coordinated to the magnesium ion and the positive charge is compensated by the sulfate(VI) anion (Figure 2). In the corresponding cobalt and cadmium complexes, the charge of the metal ions is compensated by anionic quinolone molecules. Metal–oxygen distances in magnesium complex **2** are shorter than in the corresponding Co [Co–O(1) 2.166(9) Å; Co–O(11) 2.182(8) Å] and Cd [Cd–O(1) 2.260(2) Å; Cd–O(11) 2.259(14) Å] complexes of cinoxacin.

In both compounds where two quinolone molecules are coordinated to magnesium, **1** and **4**, respectively, there is no substantial difference in Mg–O(quinolone) bond lengths (Table 4).[12,13] Not surprisingly, Mg–O(quinolone) bond lengths in compound **2** are substantially different. We assume that these differences between the complexes arise for geometrical reasons. The structure of **1** is centrosymmetric. Two quinolone molecules are arranged *trans* to each other and there is a square planar arrangement of quinolone oxygen atoms coordinated to magnesium. Aqua ligands are coordinated in the remaining axial positions. In **2**, three quinolone molecules are coordinated to magnesium. In order to adopt an octahedral arrangement of quinolone oxygen atoms around the metal center the bond lengths and angles in the coordination sphere should be different. The carboxylate group of the ciprofloxacin ligand indicated by C is slightly moved out of the plane of the aromatic quinolone part of ligand C. There is also a free mobility of the single C(1C)–C(3C) bond with which the carboxylate group is attached to the quinolone ring system. These two effects lead to the O(11C) atom being 0.764(3) Å out of the quinolone plane C. Contrary to this, the O(11A) and O(11B) atoms lie in the plane of aromatic rings A and B, respectively.

Appearance of the Quinolone Molecule in the Crystal Structures

The appearance of ciprofloxacin in the crystal structures depends on the pH of the solution.[6] It can be present as a cation, neutral molecule, or an anion (see Scheme 3). In acidic conditions the ligand could be protonated, bearing

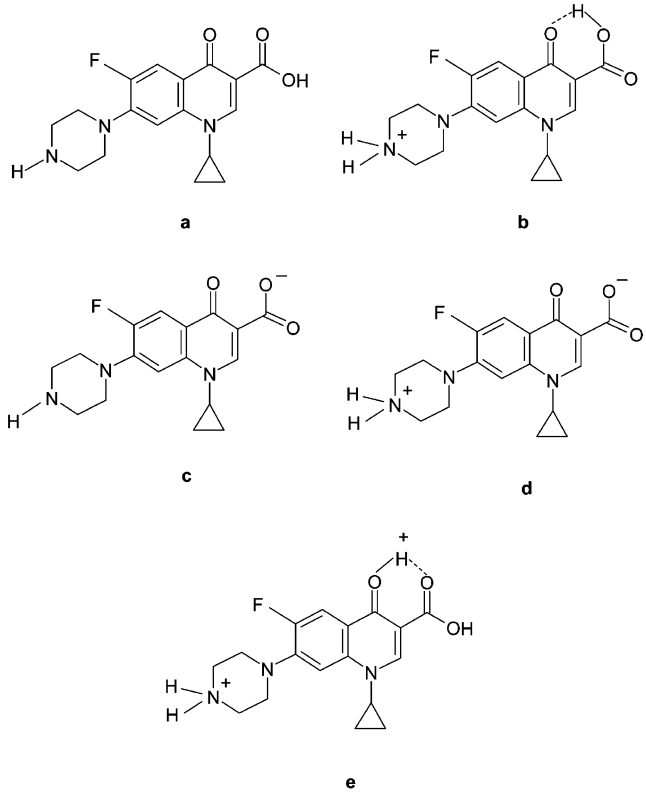

Scheme 3. Formula of cfH (**a**) and its various forms present in crystal structures. Protonated form cfH_2^+ (**b**), showing also the intramolecular hydrogen bond (present for example in ciprofloxacin hydrochloride[35] and **3**[18]). Anionic form (**c**) (present for example in **4**[13]). Zwitterionic form (**d**) (present for example in **1** and **2**). Doubly protonated form (**e**) (present for example in **5**[36]).

the charge 1+ or even 2+.[18,35,36] Typical examples containing the protonated ligand are **3** and $(cfH_2)(cfH_3)[CuCl_4]$-$Cl{\cdot}H_2O$ (**5**).[36] The charge of quinolone in **3** is 1+ since the terminal nitrogen atom of the piperazine ring is protonated but also hydrogen is bonded to the oxygen atom of the carboxylic group (see Scheme 3, b). In **5**, isolated in highly acidic media, two types of ciprofloxacin molecules are present: mono and doubly protonated. The former with charge 1+ is the same as the one described in compound **3**, whereas in the latter the charge is 2+. In this form both the nitrogen atom of the piperazine ring and also the ring carbonyl oxygen O(1) are protonated (see Scheme 3e). Quite frequently a neutral zwitterionic form of ciprofloxacin is present in the structures. The carboxylate group is deprotonated and the proton is attached to the terminal nitrogen atom of the piperazine ring. In the newly isolated complexes **1** and **2** such a form is present (see Scheme 3d). Finally, this ligand can also be coordinated to the metal as an anion if the pH is sufficiently high (slightly basic), as found in **4** (see Scheme 3c).[12,13]

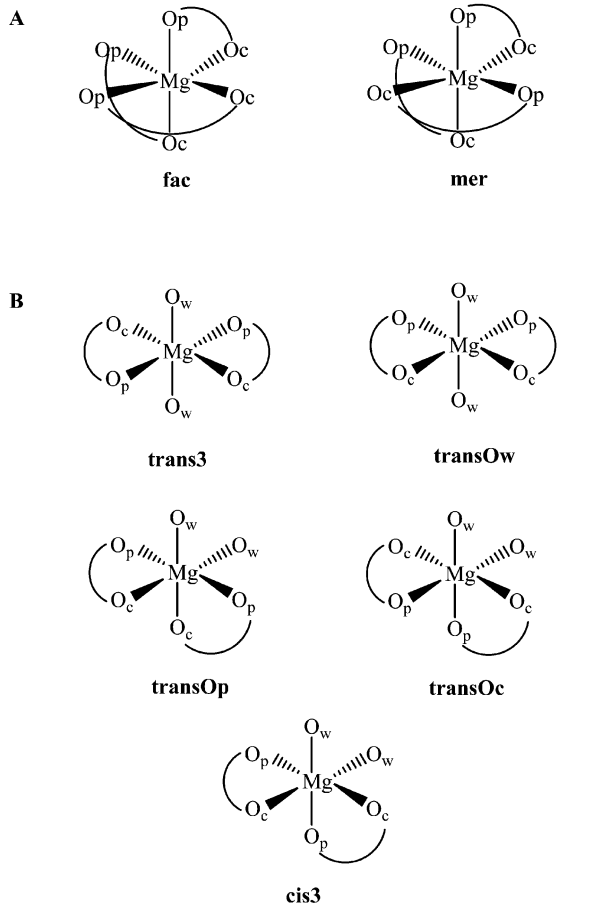

Scheme 4. The isomers of (A) $[Mg(cfH)_3]^{2+}$ and (B) $[Mg(H_2O)_2$-$(cfH)_2]^{2+}$ employed in the simulated annealing calculations. Oc and Op are the carboxylate and the pyridone oxygen atoms, respectively, of ciprofloxacin.

Molecular Dynamics of Magnesium–Ciprofloxacin Compounds

In order to investigate the energy of the structure of Mg–cfH complexes (Mg:cfH ratio from 1:1 to 1:3) and how these structures are influenced, the lowest energy model structures of $[Mg(cfH)_3]^{2+}$, $[Mg(cfH)_2(H_2O)_2]^{2+}$, and $[Mg(cfH)(H_2O)_4]^{2+}$ have been determined with molecular modeling calculations.

$[Mg(cfH)_3]^{2+}$

In order to present a model for the complex we have constructed two *fac*- and two *mer*-$[Mg(cfH)_3]^{2+}$ enantiomers (Scheme S1). The average energy of each set of enantiomers is almost equal, as is expected from such molecular mechanics calculations.[37,38] However, the final structures of *mer*-$[Mg(cfH)_3]^{2+}$ exhibit lower energies by 0.4 kcal mol^{-1} in comparison to the energies of the *fac* isomers (Table S2). For the *mer* models we applied a set of harmonic restraints at the Mg^{II}–O bonds[13,14,39–45] during an additional minimization phase (Table S3). On the basis of these results we present the lowest energy model of one *mer*-$[Mg(cfH)_3]^{2+}$ enantiomer as the most favorable configuration of the complex (Scheme 4A). The lowest energy model structure found is illustrated in Figure S1. However, we can neither exclude nor unambiguously distinguish between the favorable enantiomers.

The results obtained for the lowest energy model structure of $[Mg(cfH)_3]^{2+}$ (a *mer*-isomer) are in accordance with the X-ray crystal structure and with the lowest energy model structures of similar $[M(quinolone)_3]$ ($M = Fe^{3+}$) complexes reported in the literature.[46–48]

$[Mg(H_2O)_2(cfH)_2]^{2+}$

Ten diastereoisomers as starting models of $[Mg(H_2O)_2$-$(cfH)_2]^{2+}$ have been constructed (Scheme S2). The total number of all the possible diastereoisomers could not be limited. Although the two Ow atoms lie at *trans* positions in most similar Mg^{II} complexes,[39–43] their arrangement at *cis* positions has also been reported for a few similar Mg^{II} complexes[44,45] and cannot be ruled out. After the Langevin dynamics simulated annealing calculations, we obtained the total energy results of 20 different conformations for each starting model (Table S4). The average energy of each set of enantiomers is almost equal, as is expected from such molecular mechanics calculations.[37,38] However, the final structures of the *transOw* isomers (Scheme 4B) exhibit lower average energies by more than 2.3 kcal mol^{-1} than the other four isomers (*cis3*, *transOc*, *trans3*, and *transOp* isomers, Scheme 4B).

Applying the distance restraints (Table S5) to Mg^{II}–O bonds[13,14,39–45] for the *transOw* model with the lowest energy and making corrections to the geometry by minimizing the energy of the complex once again, the structure of the

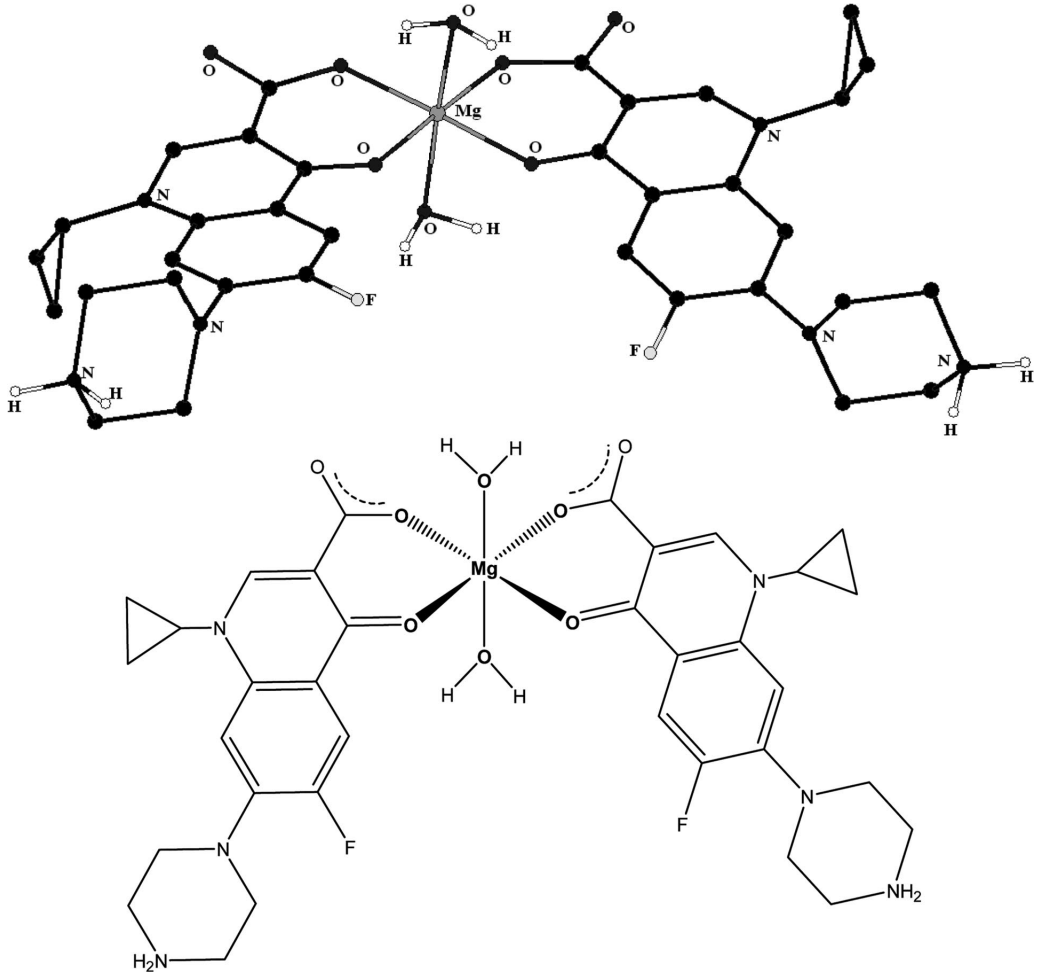

Figure 6. Lowest energy model of $[Mg(H_2O)_2(cfH)_2]^{2+}$.

predicted most stable isomer (a *transOw* isomer) has been obtained (Figure 6).

On the other hand, the *trans3* isomers exhibit the highest average energy by more than 0.7 kcal mol^{-1} than the other isomers. The results derived from the molecular modeling calculations for complex $[Mg(H_2O)_2(cfH)_2]^{2+}$ (Figure 6) are not in accordance with the crystal structure determined with X-ray crystallography. Indeed, the crystal structure of $[Mg(H_2O)_2(cfH)_2]^{2+}$ corresponds to the isomer with the highest average energy (*trans3* isomer).

The isolation of the crystals with the *trans3* configuration (as found in **1**) could be attributed to the existence of the two nitrate anions, which contribute significantly to the stabilization of the structure of the dicationic complex $[Mg(H_2O)_2(cfH)_2]^{2+}$. The contribution of the nitrate anions to the average energy of the complex has not been taken into account in the calculations because the number of all the possible resultant isomers would be dramatically increased and more complicated calculations would be required.

$[Mg(H_2O)_4(cfH)]^{2+}$

The intracellular concentration of magnesium ions is much higher than that of the quinolone drug.[2,49] It could be therefore estimated from stability constants data[50] and pKa values[51] that the amount of 1:1 magnesium–quinolone complex in solution at physiological pH is higher than that of 1:2 complex. In a 1:1 metal–quinolone complex the metal site is more exposed than in complexes with more quinolones bonded to the metal. We can also propose that the 1:1 complex interacts more easily with its biological target(s) than a 1:2 or 1:3 magnesium–quinolone complex due to steric reasons.[20] These are the main reasons why we have decided to prepare also a model of a 1:1 magnesium–quinolone complex.

For the $[Mg(H_2O)_4(cfH)_2]^{2+}$ complex, only one arrangement of the ligand atoms around Mg^{II} is possible, since the environment around Mg^{II} consists of four Ow, one Oc, and one Op atoms. So we have tried to determine the lowest energy model structure of the complex by calculating the

average energy of all the possible isomers resulting from the typical distortion modes of the octahedron, i.e. compression (*comp*) or elongation (*elong*) along each axis, distortion along the different bond lengths between Mg–Oc, Mg–Op, and Mg–Ow derived from the literature (*dist*) and, of course, the regular (*reg*) octahedron.

In this context, we have constructed 16 diastereoisomers as starting models of $[Mg(H_2O)_4(cfH)]^{2+}$ (Scheme S3). After the Langevin dynamics simulated annealing calculations, we obtained the total energy results of 20 different conformations for each starting model (Table S6). The average energy of each set of enantiomers is almost equal, as is expected from such molecular mechanics calculations.[37,38] However, the final structures of the isomers with Oc and Op at shorter distances to Mg (*elong OwOw* and *dist OpOc* isomers, Scheme S3) exhibit lower average energies by more than 1 kcal mol^{-1} than the other isomers (*comp OwOp*, *comp OwOc*, *comp OwOw*, *elong OwOc*, *elong OwOp*, and *reg*, Scheme S3).

The difference between the average total energy of *elong OwOw* and *dist OpOc* isomers is ca. 0.25 kcal mol^{-1} with the two *elong OwOw* enantiomers being more stable since they exhibit the lowest energy and the structure of the predicted most stable isomer (an *elong OwOw* isomer) has been obtained and is presented in Figure 7.

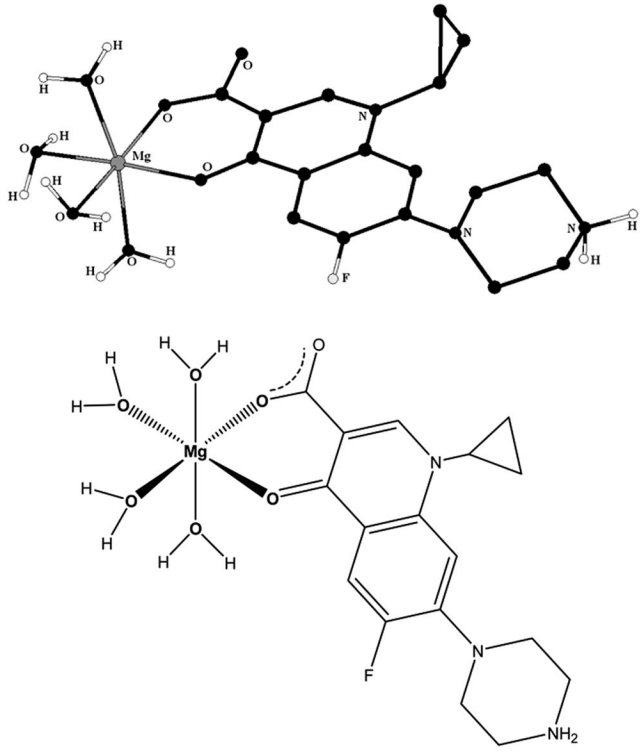

Figure 7. Lowest energy model of $[Mg(H_2O)_4(cfH)]^{2+}$.

Conclusions

Crystallographic results show that coordination of ciprofloxacin to magnesium is indeed versatile but all complexes bear a common feature—a chelate bonding of quinolone through the ring carbonyl and carboxylate oxygen atoms. The variety of complexes isolated brings us to the conclusion that it is very difficult to establish which of these complexes may be the most important for the activity of quinolones or interactions with biomolecules. The understanding of the relationship between the structure of a molecule and its biological activity is one of the central themes of medicinal chemistry. The lowest energy model structure of the 1:3 complex derived from the molecular modeling calculations is in accordance with the crystal structure determined with X-ray crystallography. On the other hand, the crystal structure of the 1:2 complex has exhibited the highest average energy in the molecular modeling calculations and its isolation could be attributed to the existence of two nitrate anions. Finally, for the 1:1 complex the structure of the most stable isomer predicted from the molecular modeling calculations has been proposed.

Our attempts to prepare appropriate crystals and to determine the crystal structure of the magnesium–quinolone complex with DNA have not been successful so far. Our metal–quinolone crystal and molecular modeling data could be very useful in further theoretical studies, especially in modeling interactions of magnesium complexes with biomolecules. Our efforts are currently also directed at studying the experimental and theoretical charge density of various metal–quinolone complexes. We believe that all these studies can elucidate the complex mechanism of action of quinolone drugs and the role of metal ions in these processes.

Experimental Section

Syntheses

$[Mg(H_2O)_2(cfH)_2](NO_3)_2·2H_2O$ (1): A Teflon reaction vessel was filled with water (5.0 mL). Under stirring, equimolar quantities (0.314 mmol) of $Mg(NO_3)_2·6H_2O$ (0.0805 g), ZnO (0.0256 g), and ciprofloxacin (0.104 g) were added. The pH of the suspension was approximately 7. The reaction vessel was closed with a lid, transferred into an autoclave, and heated at 130 °C for 22.5 h. White precipitate was filtered from the resulting suspension. Yellow mother liquor solution was transferred into a beaker. After two months of slow isothermal evaporation a small amount of orange-brown crystals of **1** appeared in the solution. Yield (based on $Mg(NO_3)_2·6H_2O$): 16.6 mg (6.0%). FTIR (*m*-medium, s-strong, b-broad): $\tilde{\nu}$ = 3443 (m, b), 3075 (m), 1621 (s), 1568 (m), 1490 (m), 1450 (m), 1414 (s), 1390 (s), 1335 (m), 1300 (s), 1274 (m), 1256 (s), 1179 (m), 1147 (m), 1133 (m), 1110 (m), 1066 (m), 1033 (m), 944 (m), 916 (m) 898 (m), 860 (m), 838 (m), 821 (s), 790 (m), 745 (s), 710 (m), 662 (m), 627 (m) cm^{-1}.

$[Mg(cfH)_3](SO_4)·5H_2O$ (2): The title compound was synthesized by a hydrothermal reaction from a mixture of cfH (0.132 g, 0.400 mmol) and magnesium sulfate heptahydrate (0.0914 g, 0.400 mmol) in water (3.0 mL). The suspension (pH = 6) was stirred and placed in a glass tube, which was then frozen by liquid nitrogen, evacuated and sealed. The ampoule was heated at 150 °C for 24 h and was slowly cooled in air. A small amount of pale violet crystals suitable for X-ray structure determination had grown on the top of a larger amount of the white microcrystalline complex

mixture after a month. Yield (based on $MgSO_4 \cdot 7H_2O$): 17.3 mg (3.6%). FTIR (*m*-medium, s-strong, b-broad): $\tilde{\nu}$ = 3379 (m, b), 1614 (s), 1577 (m), 1479 (m), 1452 (m), 1374 (m), 1359 (s), 1332 (m), 1305 (m), 1291 (s), 1256 (s), 1177 (m), 1145 (m), 1103 (m), 1041 (m), 1023 (m), 940 (m), 892 (m), 862 (m), 832 (m), 819 (s), 784 (m), 744 (s), 729 (s), 710 (m), 620 (s) cm^{-1}.

Infrared Spectroscopy: Infrared spectra were recorded with a Perkin–Elmer Spectrum 100 FT-IR spectrometer, equipped with a Specac golden gate diamond ATR as a sample support.

Crystallography: X-ray crystallographic data of compounds **1** and **2** are summarized in Table 1. Intensity data were collected at 293 K for **1** and 150 K for **2**, respectively on Nonius Kappa CCD diffractometers equipped with a cooling device (Oxford Cryosystems, Cryostream Cooler), a Mo anode (λ = 0.71073 Å), and a graphite monochromator. A multiscan absorption correction was performed.[52] The structures were solved by direct methods (SIR-97[53] for **1** and SHELXS-97[54] for **2**) and refined by a full-matrix least-squares procedure based on F^2 (SHELXL-97).[55] Hydrogen atoms attached to water oxygen atoms and piperazine nitrogen atoms were found in difference Fourier maps and were refined freely. All the remaining H atoms were placed at calculated positions and treated using appropriate riding models.

CCDC-682988 (for **1**) and -682989 (for **2**) contain the supplementary crystallographic data. These data can be obtained free of charge from The Cambridge Crystallographic Data Centre via www.ccdc.cam.ac.uk/data_request/cif.

Molecular Modeling: With the aim to present a molecular model for each complex that is unbiased by the starting structure, we have used Langevin dynamics with a simulated annealing protocol. Using this method, the mean total energy of an ensemble of structures guides the selection of the most favorable configuration for each complex. Starting structures were constructed using the program HyperChem and the MM+ force field that is based on Allinger's MM2 force field.[56] For magnesium ions we used a default parameter set with R* = 2.20 Å and e* = 0.02 kcal mol^{-1}, since their van der Waals interactions are not expected to play a major role in such bonded representations as in octahedral complexes. Mg–O bond lengths were corrected in the final models using harmonic restraints with equilibrium values that were extracted from crystallographic data of similar compounds[13,14,39–45] (Tables S3, S5 and Scheme S3). Nonbonded interactions were calculated in vacuo with no cutoff and the electrostatic energy term was treated using bond dipoles. Initial energy minimizations were carried out by a conjugate gradient method with rms gradient <0.01 as convergence criterion.

Each model (Schemes S1, S2, S3) was subjected to 20 individual rounds of simulated annealing setting different values to the seed for the assignment of the starting velocities. To integrate the Langevin equation[57] the step size was set to 1 fs and the collision frequency to 1 ps^{-1}. The annealing calculation comprised three phases: (i) raising the temperature of the system from 10 to 1000 K over 2 ps, (ii) keeping the system at 1000 K for 3 ps and (iii) cooling the system down to 0 K over 15 ps. A tight coupling of the system with temperature (0.1 ps) was used for the heating and equilibration phases. During the cooling phase the bath relaxation time was gradually decreased from 5.0 ps (7000 steps), 2.0 ps (3000 steps), 1.0 ps (2000 steps), 0.5 ps (2000 steps) to 0.05 ps (1000 steps). At the final step all structures had rms gradient <0.01 and their total energy was recorded (Tables S2, S4, S6). The models presented herein were selected among the lowest energy structures that were generated for each starting geometry. A final minimization of their energy was performed as above, but having applied the metal–ligand distance restraints.

Supporting Information (see footnote on the first page of this article): Hydrogen bonding geometry for **1** and **2** (Table S1). Three schemes (Schemes S1–S3) for the diastereoisomers of $[Mg(cfH)_3]^{2+}$, $[Mg(H_2O)_2(cfH)_2]^{2+}$, and $[Mg(H_2O)_4(cfH)]^{2+}$ employed in the simulated annealing calculations, three Tables (Table S2, S4, S6) for the energy statistics from the simulated annealing results of $[Mg(cfH)_3]^{2+}$, $[Mg(H_2O)_2(cfH)_2]^{2+}$, and $[Mg(H_2O)_4(cfH)]^{2+}$ diastereoisomers, two Tables (Tables S3, S5) for the metal–ligand distance restraints applied during the energy-minimizing phase in order to adjust the geometry of $[Mg(cfH)_3]^{2+}$ and $[Mg(H_2O)_2(cfH)_2]^{2+}$ models and one Figure (Figure S1) of the lowest model structure of $[Mg(cfH)_3]^{2+}$.

Acknowledgments

This work was supported by the Slovenian Ministry of Higher Education, Science and Technology (MHEST), project P1-0175. S. T. is grateful to the Socrates Erasmus Exchange Program for a grant.

[1] L. A. Mitscher, *Chem. Rev.* **2005**, *105*, 559–592.
[2] K. E. Brighty, T. D. Gootz in *The Quinolones* (Ed.: V. T. Andriole), Academic Press, San Diego, **2000**, pp. 33–97.
[3] G. Sheehan, N. S. Y. Chew in *Fluoroquinolone Antibiotics* (Eds.: A. R. Ronald, D. E. Low), Birkhauser, Basel, Switzerland, **2003**, p. 1–10.
[4] S. W. Glickman, E. B. Rasiel, C. D. Hamilton, A. Kubataev, K. A. Schulman, *Science* **2006**, *311*, 1246–1247.
[5] Y. L. Janin, *Bioorg. Med. Chem.* **2007**, *15*, 2479–2513.
[6] I. Turel, *Coord. Chem. Rev.* **2002**, *232*, 27–47, and the references cited therein.
[7] P. Drevenšek, I. Turel, N. Poklar Ulrih, *J. Inorg. Biochem.* **2003**, *96*, 407–415.
[8] N. Jimenez-Garrido, L. Perello, R. Ortiz, G. Alzuet, M. Gonzalez-Alvarez, E. Canton, M. Liu-Gonzalez, S. Garcia-Granda, M. Perez-Priede, *J. Inorg. Biochem.* **2005**, *99*, 677–689.
[9] P. B. Pansuriya, P. Dhandhukia, V. Thakkar, M. N. Patel, *J. Enzyme Inhib. Med. Chem.* **2007**, *22*, 477–487.
[10] M. E. Katsarou, E. K. Efthimiadou, G. Psomas, A. Karaliota, D. Vourloumis, *J. Med. Chem.* **2008**, *51*, 470–478.
[11] Z. F. Chen, R. G. Xiong, J. L. Zuo, Z. Guo, X. Z. You, H. K. Fun, *J. Chem. Soc., Dalton Trans.* **2000**, 4013–4014.
[12] D. R. Xiao, E. B. Wang, H. Y. An, Z. M. Su, Y. G. Li, L. Gao, C. Y. Sun, L. Xu, *Chem. Eur. J.* **2005**, *11*, 6673–6686.
[13] P. Drevenšek, N. Poklar Ulrih, A. Majerle, I. Turel, *J. Inorg. Biochem.* **2006**, *100*, 1705–1713.
[14] P. Drevenšek, J. Košmrlj, G. Giester, T. Skauge, E. Sletten, K. Sepčić, I. Turel, *J. Inorg. Biochem.* **2006**, *100*, 1755–1763.
[15] G. Palu, S. Valisena, G. Ciarocchi, B. Gatto, M. Palumbo, *Proc. Natl. Acad. Sci. USA* **1992**, *89*, 9671–9675.
[16] C. Sissi, E. Perdona, E. Domenici, A. Feriani, A. J. Howells, A. Maxwell, M. Palumbo, *J. Mol. Biol.* **2001**, *311*, 195–203.
[17] C. J. R. Willmott, A. Maxwell, *Antimicrob. Agents Chemother.* **1993**, *37*, 126–127.
[18] I. Turel, I. Leban, M. Zupančič, P. Bukovec, K. Gruber, *Acta Crystallogr., Sect. C* **1996**, *52*, 2443–2445.
[19] I. Turel, J. Golič, O. L. R. Ramirez, *Acta Chim. Slov.* **1999**, *46*, 203–211.
[20] J. Overgaard, I. Turel, D. E. Hibbs, *Dalton Trans.* **2007**, 2171–2178.
[21] I. Turel, N. Bukovec, E. Farkas, *Polyhedron* **1996**, *15*, 269–275.
[22] P. Drevenšek, T. Zupančič, B. Pihlar, R. Jerala, U. Kolitsch, A. Plaper, I. Turel, *J. Inorg. Biochem.* **2005**, *99*, 432–442.
[23] I. Turel, A. Golobič, A. Klavžar, B. Pihlar, P. Buglyó, E. Tolis, D. Rehder, K. Sepčić, *J. Inorg. Biochem.* **2003**, *95*, 199–207.

[24] N. C. Baenziger, C. L. Fox, S. L. Modak, *Acta Crystallogr., Sect. C* **1986**, *42*, 1505–1509.
[25] I. Turel, I. Leban, N. Bukovec, *J. Inorg. Biochem.* **1994**, *56*, 273–282.
[26] I. Turel, K. Gruber, I. Leban, N. Bukovec, *J. Inorg. Biochem.* **1996**, *61*, 197–212.
[27] D. Čurman, P. Živec, I. Leban, I. Turel, A. Polishchuk, K. D. Klika, E. Karaseva, V. Karasev, *Polyhedron* **2008**, *27*, 1489–1496.
[28] A. G. Orpen, L. Brammer, F. H. Allen, O. Kennard, D. G. Watson, R. Taylor, *J. Chem. Soc., Dalton Trans.* **1989**, S1–S83.
[29] F. H. Allen, O. Kennard, D. G. Watson, L. Brammer, A. G. Orpen, R. Taylor, *J. Chem. Soc. Perkin Trans. 2* **1987**, S1–S19.
[30] L. J. Barbour, G. William Orr, J. L. Atwood, *Nature* **1998**, 393–671.
[31] P. Ball, *Chem. Rev.* **2008**, *108*, 74–108.
[32] W. Massa, O. V. Yakubovich, O. V. Dimitrova, *Acta Crystallogr., Sect. C* **2003**, *59*, i83–i85.
[33] C. Chulvi, M. C. Muñoz, L. Perelló, R. Ortiz, M. I. Arriortua, J. Via, K. Urtiaga, J. M. Amigó, L. E. Ochando, *J. Inorg. Biochem.* **1991**, *42*, 133–138.
[34] M. P. Lopez-Gresa, R. Ortiz, L. Perello, J. Lattore, M. Liu-Gonzalez, S. Garcia-Granda, M. Perez-Priede, E. Canton, *J. Inorg. Biochem.* **2002**, *92*, 65–74.
[35] I. Turel, A. Golobič, *Anal. Sci.* **2003**, *19*, 329–330.
[36] P. Drevenšek, A. Golobič, I. Turel, N. Poklar, K. Sepčić, *Acta Chim. Slov.* **2002**, *49*, 857–870.
[37] P. Christofis, M. Katsarou, A. Papakyriakou, Y. Sanakis, N. Katsaros, G. Psomas, *J. Inorg. Biochem.* **2005**, *99*, 2197–2210 and references cited therein.
[38] G. Psomas, A. Tarushi, E. K. Efthimiadou, *Polyhedron* **2008**, *27*,133–138.
[39] C. C. Wagner, E. J. Baran, O. E. Piro, *J. Inorg. Biochem.* **1999**, *73*, 259–263.
[40] C. B. Case, B. M. Foxman, *Inorg. Chim. Acta* **1994**, *222*, 339–343.
[41] T. Lis, *Acta Crystallogr., Sect. C* **1992**, *48*, 424–427.
[42] J. A. Kaduk, *Acta Crystallogr., Sect. B* **2002**, *58*, 815–822.
[43] M. Gryz, W. Starosta, J. Leciejewicz, *Acta Crystallogr., Sect. E* **2006**, *62*, m123–m124.
[44] J.-P. Deloume, H. Loiseleur, G. Thomas, *Acta Crystallogr., Sect. B* **1973**, *29*, 668–673.
[45] B.-X. Liu, J.-Y. Yu, D.-J. Xu, *Acta Crystallogr., Sect. E* **2006**, *62*, m231–m232.
[46] E. K. Efthimiadou, Y. Sanakis, N. Katsaros, A. Karaliota, G. Psomas, *Polyhedron* **2007**, *26*, 1148–1158.
[47] E. K. Efthimiadou, G. Psomas, Y. Sanakis, N. Katsaros, A. Karaliota, *J. Inorg. Biochem.* **2007**, *101*, 525–535.
[48] A. Tarushi, P. Christofis, G. Psomas, *Polyhedron* **2007**, *26*, 3963–3972.
[49] S. Lecomte, M. H. Baron, M. T. Chenon, C. Coupry, N. J. Moreau, *Antimicrob. Agents Chemother.* **1994**, *38*, 2810–2816, and the references cited therein.
[50] J. Shimada, K. Shiba, T. Oguma, H. Miwa, Y. Yoshimura, T. Nishikawa, Y. Okabayashi, T. Kitagawa, S. Yamamoto, *Antimicrob. Agents Chemother.* **1992**, *36*, 1219–1224.
[51] Y. X. Furet, J. Deshusses, J. C. Pechere, *Antimicrob. Agents Chemother.* **1992**, *36*, 2506–2511.
[52] Z. Otwinowski, W. Minor, *Methods Enzymol.* **1997**, *276*, 307–326.
[53] A. Altomare, M. C. Burla, M. Camalli, G. L. Cascarano, C. Giacovazzo, A. Guagliardi, A. G. G. Moliterni, G. Polidori, R. Spagna, *J. Appl. Crystallogr.* **1999**, *32*, 115–119.
[54] G. M. Sheldrick, *SHELXS-97*, Program for Crystal Structure Determination, University of Göttingen, Germany, **1997**.
[55] G. M. Sheldrick, *SHELXL-97*, Program for the Refinement of Crystal Structures, University of Göttingen, Germany, **1997**.
[56] N. L. Allinger, *J. Am. Chem. Soc.* **1977**, *99*, 8127–8134.
[57] M. P. Allen, D. J. Tildesley (Eds.), *Computer Simulation of Liquids*, Oxford University Press, Oxford, **1989**.

Received: April 2, 2008
Published Online: July 7, 2008

